ELSEVIER

Fire Safety Journal 31 (1998) 61–75

FIRE SAFETY JOURNAL

Rheology of fire-fighting foams

B. S. Gardiner, B. Z. Dlugogorski*, G. J. Jameson

Department of Chemical Engineering, The University of Newcastle, Callaghan, NSW 2308, Australia

Received 26 July 1996; revised version received 17 June 1997; accepted 1 July 1997

Abstract

This paper examines the rheological properties of compressed-air foams and contains velocity profiles of foams flowing through straight horizontal tubes. It is shown that a master equation can be derived from the experimental data to account for a range of expansion ratios and pressures normally encountered during pumping of polyhedral-in-structure fire-fighting foams. The experimental data come from a Poiseuille-flow rheometer consisting of three stainless steel tubes 6.95, 9.9, 15.8 mm in diameter, with foam generated by mixing a pressurised solution of Class A foam with compressed air. Results are corrected for wall slip following the method of Oldroyd-Jastrzebski, which implies the dependence of slip coefficients on the curvature of the tube wall. The experimental results demonstrate the applicability of the volume equalisation method to the more expanded, polyhedral ($\varepsilon > 5$) and transition, bubbly-to-polyhedral ($5 \geqslant \varepsilon \geqslant 4$) foams. (The method of volume equalisation was introduced by Valkó and Economides to correlate the viscosity of low expansion foams ($\varepsilon < 4$), characterised by spherical bubbles.) The present results indicate that all data points align themselves along two master curves, depending on whether the foam consists of bubbles or polyhedral cells.

Keywords: Foam rheology; fire fighting foams; Poiseuille pipe rheometer; wall-slip correction; volume equalisation; power-law model

Notation

D	pipe internal diameter, m
E	expansion ratio, volume of foam/volume foam solution at atmospheric conditions, –

* Author to whom correspondence should be addressed.

0379-7112/98/$19.00
PII: S0379-7112(97)00049-0

f	friction factor, –
K	apparent power-law coefficient in Eq. (10), Pa $s^{1/n}$
k	power-law coefficient, Pa $s^{1/n}$
m_L, m_a	mass of foam solution and mass of air, respectively, contained in a given volume of foam at atmospheric conditions, kg
n	power-law exponent, –
Q, Q_{calc}	experimental and calculated volumetric flow rates, respectively, $m^3\ s^{-1}$
R	pipe internal radius, m
r	radial coordinate, m
u_{slip}	slip velocity, $m\ s^{-1}$
x	axial coordinate, m
β_c	corrected slip coefficient, $m^2\ Pa^{-1}\ s^{-1}$
$\dot{\gamma}$	non-Newtonian shear rate, s^{-1}
$\dot{\gamma}_{aw}$,$(\dot{\gamma}_{aw})_{True}$	apparent shear rate and apparent shear rate corrected for slip at the wall, s^{-1}
$\Delta P/L$	pressure drop per unit length, Pa m^{-1}
ε	specific expansion ratio, ρ_L/ρ, –
μ	viscosity, Pa s
ρ_L, ρ	density of foam solution and foam at *in situ* conditions, $kg\ m^{-3}$
τ, τ_w	shear stress and wall shear stress, respectively, Pa

Superscript

*	denotes reference state

1. Introduction

Foams possess properties which make them superior fire-suppression agents over the traditional application of water against fires. For example, liquid contained in the foam drains slowly from a foam, trapping the water at the fuel's surface and reducing inefficiency due to run-off. The surfactants lower the surface tension of the foam solution, with respect to that of water, enabling the solution to penetrate and wet porous material. This property is very useful in smothering existing fires and in mop-up operations. In addition, foams act as barriers to thermal radiation by inducing multiple scattering of infrared waves, followed by heat absorption. Foams also function as barriers to diffusion, suppressing the evolution of dangerous fumes.

The application dictates what type of foam is required in the field. Low expansion foams exhibit good wetting properties and are sprayed directly onto a fire. It has been observed that these wetter low-expansion foams are more effective against forest fires [1]. On the other hand, high expansion foams are more viscous and tend to adhere to vertical surfaces (such as walls or tree foliage). These foams can be laid by fire crews some time before the arrival of flames to absorb heat convected and radiated by the approaching fire. High expansion foams also function as a total flooding agent by

rapidly filling enclosed spaces. This particular property makes them suitable for mitigation of fires in mines and warehouses.

In recent years, traditional air-aspirated foams (generated by inducing turbulent mixing between air and foam solution inside the foam injection nozzles) are being replaced by compressed air foams (CAFs) [2]. The latter are prepared by combining flows of compressed air with foam solution away from the point of application. The advantage of CAFs comes from the fact that the ratio of air and foam solution can be adjusted according to the requirements imposed by an application. In addition, CAFs possess high injection momentum enabling them to be projected over long distances. Because of its mode of generation, away from the fire, CAFs are often passed along long stretches of fire hoses. No rheological data exist to predict the behaviour of fire-fighting foams occurring during such flows, giving us an impetus to embark on the present investigation.

In this paper, the expansion ratio (E) means the volume of foam divided by a volume of foam solution contained in the foam, at atmospheric conditions. This definition corresponds to the one included in NFPA 412 [3]. However, when foams are pumped at elevated pressures, bubbles decrease in size, reducing the volume occupied by the gas phase. To account for the compressibility effects of foam bubbles, the paper uses a specific expansion ratio (ε), defined as the ratio of the foam-solution density to the foam density, at the temperature and pressure existing during foam flow (*in situ*). If the flow occurs at atmospheric conditions, both terms E and ε are related through the expression: $\varepsilon = \rho_L/\rho = Em_L/(m_L + m_a)$. Within the context of the present work, carried out at elevated pressures, the specific expansion ratio stands as a more appropriate parameter, and so it is used throughout the paper.

Foam is a complex fluid with a macrostructure (bubbles and cells) which strongly influences its flow characteristics. This is particularly important in cases when the foam structure is comparable to the dimension of the flow channel. For specific expansion ratios below 3.8 and narrow distributions of sizes, bubbles are spherical and are free to move relative to one another. However, when the bubble size distribution broadens, bubbly foams may persist even at higher specific expansion ratios [4]. The location of the transition point between bubbly and cellular foams defines a change in foam rheology, as will be reported later in this paper.

At $\varepsilon \geqslant 4$, bubbles come into contact with their neighbours, distorting their boundaries and forming polyhedral cells. When this happens, films shared by neighbouring cells restrict the cell's relative motion. This leads to the appearance of an apparent yield stress [5–7], and to foam moving as a rigid plug which slips on a thin layer of foam solution at the pipe wall [8]. The existence of shear-thinning further complicates the rheological behaviour of foams. In the past, the interplay among yield stress, shear-thinning and slippage at the wall resulted in the geometry-dependent (apparent) viscosity data published in the literature, as reported by Heller and Kuntamukkula [9]. In particular, it was found that foam's apparent viscosity, uncorrected for slippage, depends strongly on the thickness and viscosity of the liquid boundary layer [9–12].

To describe the behaviour of foams of different liquid fractions, Valkó and Economides [13] introduced the principle of volume equalisation. On the basis of previous

investigations, these researchers observed that foam rheology depends on shear rate and one additional parameter. They hypothesised that this parameter is foam density ρ normalised with respect to the density of foam solution ρ_L; in other words $\varepsilon = \rho_L/\rho$. The principle of volume equalisation implies that the flow data for foams characterised by a range of expansions ratios (E) and pressures, can be reduced to a single equation relating foam stress to the shear rate, with the help of this single parameter ε. The present paper demonstrates how to carry out the data reduction process for expanded polyhedral ($\varepsilon > 5$) and transition, bubbly-to-cellular ($5 \geqslant \varepsilon \geqslant 4$), foams at intermediate pressures ($300 < P < 500$ kPa).

As done by Enzendorfer et al. [10], we have built a small scale pipe rheometer, also known as a Poiseuille rheometer, for studying foams. The Poiseuille rheometer has the added advantage of a simple geometry which closely resembles real applications. In conjunction with the volume equalisation principle, Enzendorfer and his co-workers collected and analysed rheological data for foams in a region of special interest to the petroleum industry, i.e. for $3 < P < 7$ MPa and for specific expansion rations between 1.9 and 3.3. However, compressed air foams used in fire fighting contain relatively more air and flow at lower pressures, i.e. $0.1 < P < 1$ MPa and $\varepsilon \geqslant 4$. From this perspective, the objective of the present work was to collect rheological data relevant to flow of fire-fighting foams and investigate whether the method of volume equalisation is applicable in this region.

2. Experimental apparatus

Fig. 1 illustrates the experimental apparatus which consists of a foam generator and pipe viscometer. Foam is produced by mixing compressed air with a surfactant solution. Results presented here were obtained using a 0.5% solution of Silv-ex Class

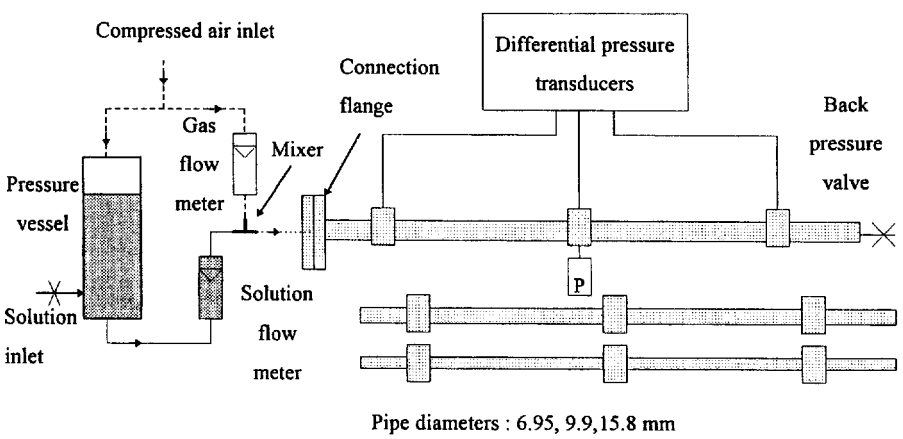

Fig. 1. Major components of the experimental apparatus.

A foam concentrate, containing butyl carbitol, ether sulfates and glycol ether. In this formulation, ether sulfates act as the surfactant, glycol ether as a stabiliser and butyl carbitol as a solvent, known for its high viscosity and low evaporation rates. This type of foam is particularly effective in suppression of fires of carbonaceous materials, and is applied extensively against forest fires. Recently, Class A compressed-air foams have also been gaining popularity for mitigation of structural fires [2].

Referring to Fig. 1, the surfactant solution is forced out of the pressure vessel by compressed air, eliminating the need for a grease-free foam-solution pump. The foam solution is later combined with compressed air in an in-line mixer. The mixer consists of compacted steel wool placed in a T-junction and is followed by a foam improver. Foam flow rates and expansion ratios are determined from flow-meter and pressure-gauge readings, and are verified by weighing the foam at atmospheric pressure, as described in NFPA 412 [3]. The present system generates foams, with expansion ratios of up to 40, characterised by a narrow distribution of bubble sizes. At atmospheric conditions, the foam texture is similar to shaving cream, as is that investigated by Durian et al. [14]. Average bubble and cell diameters have not been measured, but are estimated on the basis of Durian et al.'s results to be around 100 μm.

The Poiseuille flow rheometer consists of three separate stainless steel tubes, 1400 mm in length, and 6.95, 9.9, 15.8 mm in diameter. This selection of pipe diameters allows investigation of a large range of flow rates and pressures, and permits the data to be corrected for wall slip. Differential pressure transducers record pressure drops over 0.5 and 1 m pipe sections. A pressure gauge is located midway between transducer ports to provide average pressure readings. Each pressure port interfaces with the foam by a 0.5 mm in-diameter hole to minimise disturbances to the foam flow. Entrance effects are eliminated by measuring pressure drops over pipe sections located away from the pipe's inlet and exit. Note that the foam pumping velocities are of the order of 2 m/s, well below the velocity of sound estimated to be around 60 m/s. This means that there is no effect of exit on pipe flow from compression shock waves when the foam eventually emerges from the apparatus.

3. Data reduction

Table 1 lists the experimental conditions at which the results were obtained. All experiments were performed at constant room temperature, i.e. $20 \pm 2°C$. Note that pressure settings and expansion ratios of foams were varied independently. Calculations in the subsequent sections of the paper will demonstrate that foam rheology depends on the specific expansion ratio, ε, a parameter computed both from the *in situ* readings of pressure and temperature, and from the knowledge of expansion ratio E measured at atmospheric conditions.

To illustrate the data reduction process, the results derived directly from the experimental data, such as the volumetric flow rate Q and pressure drop ΔP, are tabulated below. The apparent Newtonian shear rate and stress at the rheometer's

Table 1
List of parameters altered in each experimental series to investigate the effects of pressure and expansion ratio on foam rheology

No.	Pressure, P (kPa)	Expansion ratio, E	Specific expansion ratio, ε
1	340	30.4	7.5
2	340	25.5	6.5
3	340	20.3	5.6
4	340	15.8	4.4
5	440	31.7	6.7

wall come from the following expressions:

$$\dot{\gamma}_{aw} = \frac{32Q}{\pi D^3}, \tag{1a}$$

and

$$\tau_w = \frac{D\Delta P}{4L}. \tag{1b}$$

Fig. 2 displays the relationship between the nominal Newtonian shear rate and the stress at the wall, using the data assembled in Table 2. It is apparent in Fig. 2 that there is a discontinuity in the flow curves when diameters change. This shift to higher shear rates with smaller diameters is due to wall slippage. The next section will demonstrate how to eliminate this geometry dependence from the flow data by introducing a correction for the wall slip.

3.1. Slip correction

Many polymer solutions, melts, gels, emulsions and dispersions exhibit slippage at the wall surface [11]. This is also true for foams. The slippage produces higher observed flow rates than true foam flow rates. In order to elucidate the rheology of bulk foam, one needs to correct the results (presented in the previous section) for this slippage. This is done by applying the method of Oldroyd [15], as implemented by Jastrzebski [12] for the reduction of the rheological measurements obtained from a system of concentrated suspensions of kaolinite. The Oldroyd–Jastrzebski correction differs from the Mooney correction [16] in that it recognises that for structured fluids the slip velocity depends on wall curvature [12]:

$$\beta = \frac{\beta_c}{D} = \frac{u_{slip}}{\tau_w} \tag{2}$$

where β_c is the corrected slip coefficient which varies only with wall stress, but not with the diameter of the tube. The Oldroyd–Jastrzebski correction found its particular use for slurries and has recently been applied to foams [10].

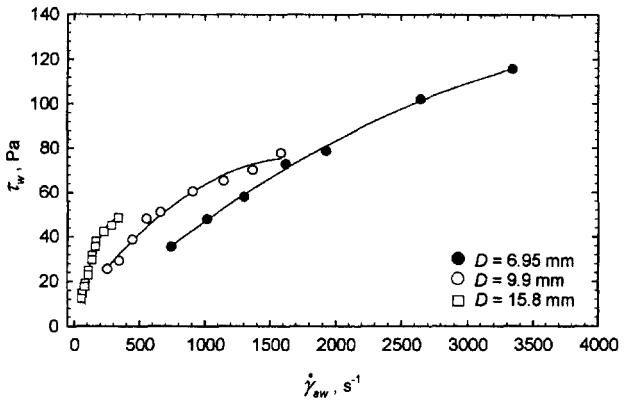

Fig. 2. Effect of the diameter-dependent slippage at the wall on the foam flow curves, as derived from experimental results at $P = 340$ kPa and $E = 25.5$.

Table 2
A sample of rheological results obtained at $P = 340$ kPa and $E = 25.5$. These conditions correspond to series 2 in Table 1

$D = 6.95$ mm		$D = 9.9$ mm		$D = 15.8$ mm	
$\dot{\gamma}_{aw}$, s^{-1}	τ_w, Pa	$\dot{\gamma}_{aw}$, s^{-1}	τ_w, Pa	$\dot{\gamma}_{aw}$, s^{-1}	τ_w, Pa
743	35.6	255	25.6	64	14.5
1016	48.0	348	29.3	87	18.9
1304	58.0	447	38.7	112	24.8
1617	73.0	554	47.9	139	31.5
1925	78.9	660	51.1	165	35.5
2647	102.2	908	60.6	168	37.8
3340	115.7	1145	65.3	227	42.2
		1367	70.3	286	44.9
		1583	78.0	342	48.5

The observed flow rate incorporates the true flow rate due to the flow of foam itself and a component due to apparent slip:

$$(Q)_{\text{Observed}} = (Q)_{\text{True}} + (Q)_{\text{Slip}} \tag{3a}$$

or

$$(Q)_{\text{Observed}} = (Q)_{\text{True}} + \left(\frac{\pi D \tau_w \beta_c}{4}\right). \tag{3b}$$

By multiplying Eq. (3b) by $32/(\pi D^3)$, the following expression is obtained:

$$\dot{\gamma}_{aw} = (\dot{\gamma}_{aw})_{\text{True}} + \frac{8\tau_w \beta_c}{D^2}. \tag{4}$$

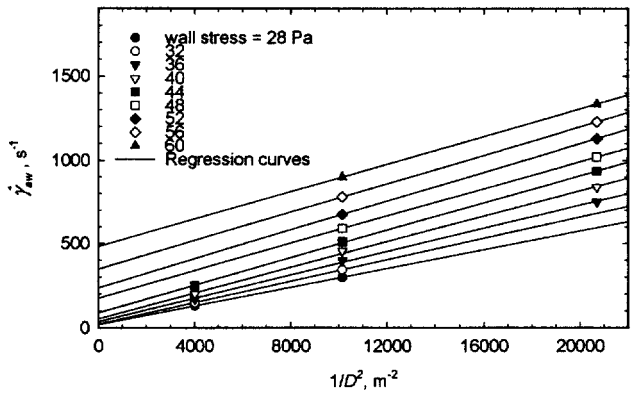

Fig. 3. Oldroyd–Jastrzebski construction for determining slip coefficients; $E = 25.5$, $P = 340$ kPa. Mooney correction applied to the same data leads to nonphysical results of negative shear rates at large pipe diameters, as observed by others as well [10].

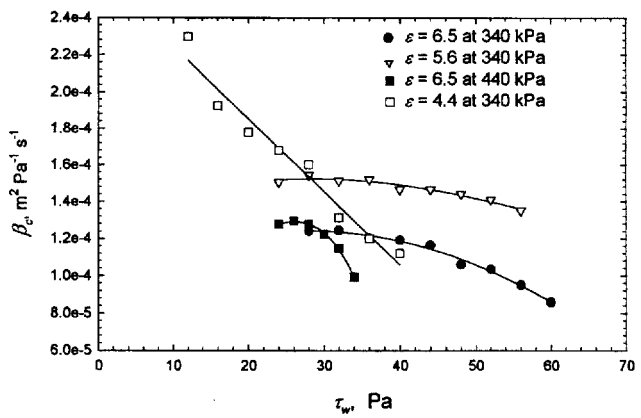

Fig. 4. Observed dependence of corrected slip coefficient on the wall shear stress for cellular foams at intermediate pressures. The results shown in Figs 2 and 3 correspond to $\varepsilon = 5.6$ and $P = 340$ kPa. Note the behaviour of β_c at higher pressures ($\varepsilon = 6.5$ and $P = 440$ kPa) and for foams in the transition bubbly-to-cellular region ($\varepsilon = 4.4$ and $P = 340$ kPa).

Figs. 3 and 4 illustrate the Oldroyd–Jastrzebski correction depicting stages of its implementation, as applied to data in Fig. 2. A plot of the apparent wall shear rate against the reciprocal of the square of pipe diameter (Fig. 3), for constant τ_w, gives the corresponding corrected wall slip coefficients as slopes of the least-squares straight lines divided by $8\tau_w$. The results illustrated in Fig. 3 are physically meaningful since the extrapolation of straight lines to very large pipe diameters ($1/D^2 \to 0$) gives positive values of the corrected Newtonian shear rates $(\dot{\gamma}_{aw})_{True}$.

The dependence of β_c on τ_w for polyhedral ($\varepsilon > 5$) and transition ($5 \geqslant \varepsilon \geqslant 4$) foams at intermediate pressures ($300 < P < 500$ kPa) can now be seen in Fig. 4. Note that the lines of best fit are not straight, but exhibit plateaux at low stress. However, it is particularly interesting to observe that for foams studied in the present investigation, the corrected slip coefficients decline with increasing stress. In other studies, which also rely on the Oldroyd–Jastrzebski correction, the opposite observations were reported; see for example ref. [10] for bubbly foams and ref. [12] for concentrated suspensions.

From the physical perspective it is not at all unreasonable to expect a declining β_c. This is because the stress-dependence of the slip coefficient is determined by the microstructural arrangement occurring in the flowing material, which may enhance or slow down the rate of increase of the slip velocity, with respect to the imposed stress. Although the exact explanation of the observed phenomenon has not been elucidated at present, the following may contribute to this behaviour of β_c: (i) as the foam flows faster through the tube, an insufficient amount of foam solution is able to be released (drained) from the films and Plateau borders to allow complete formation of the wall layer; (ii) faster motion of foam may promote collisions of larger bubbles with the wall leading to the intermittent destruction of the wall layer; and finally (iii) the physical time for flow may be too fast in comparison to the relaxation time for the foam to allow the foam microstructure to adapt itself to increased stress.

The Oldroyd–Jastrzebski correction, when applied to data presented in Fig. 2, aligns all experimental points along a single flow curve, as illustrated in Fig. 5. This result confirms applicability of the Oldroyd–Jastrzebski slip correction technique at intermediate pressures for polyhedral and transition foams. However, once all experimental data are plotted on one graph, as in Fig. 6, a large spread in the results becomes immediately apparent. This indicates a need for a model which takes into account the physical state of the foam inside the pipe rheometer.

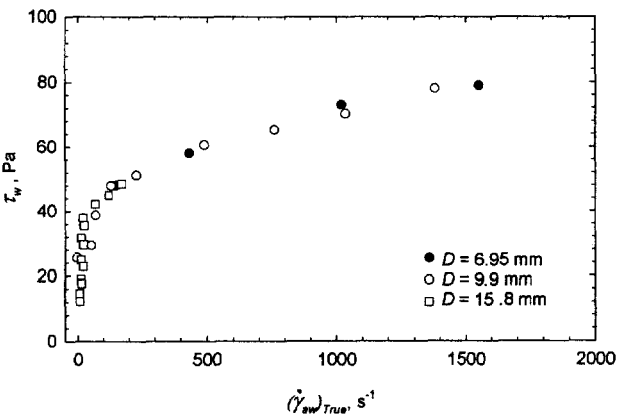

Fig. 5. Flow data corrected for wall slip; $E = 25.5$, $P = 340$ kPa.

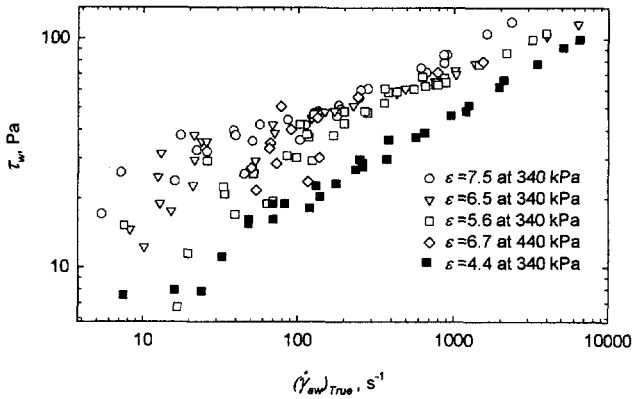

Fig. 6. Data from all experimental series, as listed in Table 1, corrected for wall slip. Note that the logarithmic plot of the results tends to add to the scatter of the data at low shear rates.

3.2. *Volume equalisation*

The method of volume equalisation is based on the observation that flow of compressible, isothermal, Newtonian fluid in a pipe of constant diameter implies a constant friction factor (the asterisk denotes a reference state whose meaning will become obvious later on):

$$f = \frac{|\tau_w^*|}{1/2u^{*2}\rho^*}. \tag{5}$$

It is immediately clear from basic fluid mechanics that, for laminar flows, f depends only on the Reynolds number $(u\rho D/\mu)$, which itself is constant; $u\rho$ is constant by continuity and μ does not vary for isothermal flows. If the expression for continuity,

$$u^* = u\frac{\rho}{\rho^*}, \tag{6}$$

is then substituted into Eq. (5), bearing in mind that f = constant, it follows,

$$\tau_w^* = \tau_w\frac{\rho}{\rho^*}. \tag{7}$$

Equation (7) provides the definition for the so-called volume-equalised wall stress [10]. If we multiply Eq. (6) by $8/D$, and generalise for any velocity and shear stress, and allow non-Newtonian behaviour, we obtain:

$$\dot{\gamma}^* = \dot{\gamma}\frac{\rho}{\rho^*}, \tag{8a}$$

and

$$\tau^* = \tau \frac{\rho}{\rho^*}, \tag{8b}$$

where the non–Newtonian

$$\dot{\gamma} = \frac{\mathrm{d}u}{\mathrm{d}r}. \tag{8c}$$

Furthermore, if the behaviour of a fluid at a reference state conforms to a power-law model, we can write:

$$\tau^* = k|\dot{\gamma}^*|^{n-1}\dot{\gamma}^*, \tag{9a}$$

or

$$\frac{\tau}{\varepsilon} = k\left|\frac{\dot{\gamma}}{\varepsilon}\right|^{n-1}\frac{\dot{\gamma}}{\varepsilon}, \tag{9b}$$

or

$$\tau = k\varepsilon^{1-n}\left|\frac{\mathrm{d}u}{\mathrm{d}r}\right|^{n-1}\frac{\mathrm{d}u}{\mathrm{d}r}. \tag{9c}$$

Equation (9b), named volume-equalised power-law [10], was obtained by replacing Eqs. (8a) and (8b) into (9a), with the foam solution itself taken as a reference state; Eq. (9c) follows from Eqs. (9b) and (8c). For the apparent slip-corrected shear rate and shear stress at the wall, the following expression is applicable for correlation of the experimental results [17]:

$$\frac{\tau_w}{\varepsilon} = K\left|\frac{(\dot{\gamma}_{aw})_{True}}{\varepsilon}\right|^{n-1}\frac{(\dot{\gamma}_{aw})_{True}}{\varepsilon}, \quad \text{where} \quad k = K\left(\frac{4n}{1+3n}\right)^n. \tag{10}$$

Once the data in Fig. 6 are volume equalised according to Eq. (10), the results trace two lines, one for polyhedral and one for transition foams, as illustrated in Fig. 7. Obviously, a transition in rheological behaviour occurs between these two types of foams. This is expected since within polyhedral foam flow is governed by hopping of cells and properties of thin films [18, 19]. On the other hand, for bubbly foams the flow is governed by motion of entire bubbles. The power law model is appropriate, however, for either foam type.

The least-squares calculations give $n = 0.29$, $K = 2.63$ and $k = 2.29$, for cellular foams. This means that viscosity of compressed air fire-fighting foams ($\mu = \tau/\dot{\gamma}$) is around 0.02–0.5 Pa s depending on the shear rate and specific expansion ratio.

4. Velocity profiles in flowing foams

Flow through tubes, with fluid experiencing changes in density, is two dimensional. However, in the case of laminar flow, which implies slow motion and good heat

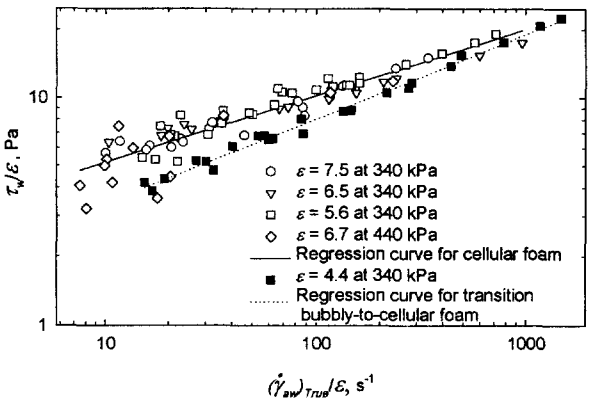

Fig. 7. Volume-equalised flow data trace two master curves, one for cellular ($\varepsilon > 5$) and one for transition ($5 \geqslant \varepsilon \geqslant 4$) foams.

transfer between the fluid and tube, flow is isothermal and the effect of changing the axial velocity on the radial velocity can be neglected [20]. Over short pipe lengths it is then possible to assume a constant pressure gradient (i.e. $\mathrm{d}p/\mathrm{d}x \approx (-\Delta p/L)$, temperature and density, and to derive the analog of the Hagen–Poiseuille formula for the volume-equalised power law.

For horizontal tubes, an elementary momentum balance around an axial cell [21] yields the following expression for shear stress:

$$\tau = \frac{\mathrm{d}p}{\mathrm{d}x}\frac{r}{2}, \tag{11a}$$

and in combination with (9c),

$$\frac{\mathrm{d}p}{\mathrm{d}x}\frac{r}{2} = k\varepsilon^{1-n}\left|\frac{\mathrm{d}u}{\mathrm{d}r}\right|^{n-1}\frac{\mathrm{d}u}{\mathrm{d}r}. \tag{11b}$$

After some manipulation [21], Eq. (11b) can be transformed to:

$$\left(-\frac{\mathrm{d}u}{\mathrm{d}r}\right)^{n} = \frac{\varepsilon^{n-1}}{2k}\left(-\frac{\mathrm{d}p}{\mathrm{d}x}\right)r. \tag{12}$$

An integration, with the boundary condition $u(r = R) = u_{\mathrm{slip}}$, gives:

$$u = u_{\mathrm{slip}} + \frac{n}{n+1}\left[\left(-\frac{\mathrm{d}p}{\mathrm{d}x}\right)\frac{R^{n+1}\varepsilon^{n-1}}{2k}\right]^{\frac{1}{n}}\left[1 - \left(\frac{r}{R}\right)^{\frac{n+1}{n}}\right]. \tag{13}$$

In addition to describing the velocity profiles in isothermal foams flowing through circular conduits of constant cross-sections, Eq. (13) provides a convenient means of calculating the total volumetric flow rate in the present experimental system. This is

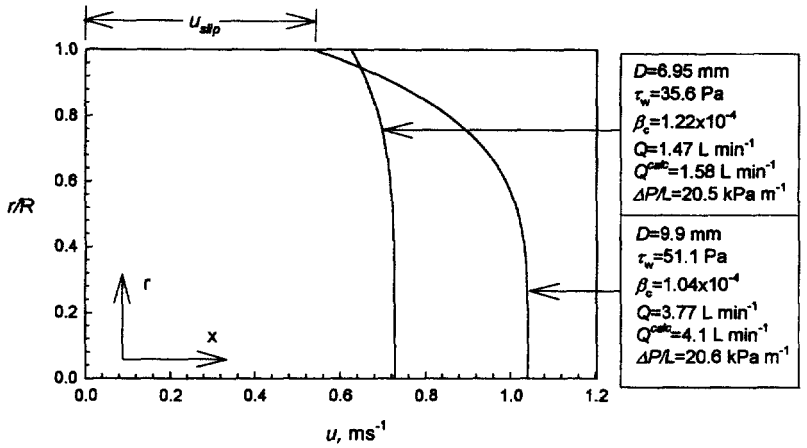

Fig. 8. Calculated velocity profiles in compressed air fire-fighting foams flowing through tubes; $P = 340$ kPa and $\varepsilon = 6.5$; β_c has units of $m^2Pa^{-1}s$.

done by integrating Eq. (13) over a cross-sectional area to obtain Q_{calc}:

$$Q^{calc} = 2\pi \int_0^R urdr = \pi R^2 \left\{ u_{slip} + \frac{n}{3n+1} \left[\left(-\frac{dp}{dx} \right) \frac{R^{n+1}\varepsilon^{n-1}}{2k} \right]^{\frac{1}{n}} \right\}. \tag{14}$$

Eq. (14) constitutes the Hagen–Poiseuille formula for volume-equalised power law, assuming negligible changes in pressure gradient, temperature and density over a short distance along the flow.

Fig. 8 compares velocity profiles [calculated from Eq. (13) and (2) in conjunction with Fig. 4] generated by the same pressure drop over 1 m sections in two tubes of different diameters. The flow in both tubes is characterised by significant apparent slip at the walls. (The apparent slip is due to a steep velocity gradient in a thin boundary layer containing foam solution.) The slip and plug-like motion dominate the flow in the smaller diameter tube. This happens because of lower shear rates existing in this pipe (than in the larger tube) for the preset pressure drop.

For the two scenarios, the total flow rates [calculated from Eq. (14)] are given in the boxes on the right-hand side of Fig. 8. These flow rates overestimate the actual foam flow rates, by 7.5 and 8.8%, respectively. Similar overestimations of the flow rates are true for other experimental data. The reasons for these small, but consistent discrepancies may be related to the assumptions, e.g. the local incompressibility, made in the derivation of the analog of the Hagen–Poiseuille formula. That is, the flow accelerates even over small pipe sections of 1 m, as used in the present work. Another possible explanation refers to the appearance of yield stress which operates on a time scale longer than the residence time of foams in the tube, so the adjustment in the foam structure is not possible. The effect of this phenomenon is an overprediction of the flow rate from Eq. (14).

5. Conclusions

The present paper has confirmed that the method of Oldroyd–Jastrzebski (as opposed to that of Mooney) for correcting flow data for apparent wall slip is appropriate for polyhedral-in-structure and transition foams ($\varepsilon \geqslant 4$) at intermediate pressures ($300 < P < 500$ kPa). This is an important observation, since compressed air foams are often used in practice in this region. The Oldroyd–Jastrzebski slip-correction method eliminates geometry dependence of foam rheology, allowing extraction of true rheological results from experiments carried out in a Poiseuille rheometer fitted with various diameter pipes.

The method of volume equalisation applied to the experimental data leads to the emergence of a master curve describing a power-law relationship between volume-equalised shear stress and volume-equalised rate of strain. However, the master curve for cellular foam differs from that obtained for transition, bubbly-to-cellular foams. This highlights dissimilar rheological (and hence microstructural) behaviour of cellular and transition foams; with the latter being less viscous than the former.

Using the equalised power-law expression, the paper illustrates velocity profiles for laminar foams flowing in tubes. The foam slips at the wall and shows an almost-flat velocity profile at the centre of the tube. This phenomena is consistent with the concept of apparent yield stress reported by others. Unlike previous investigations, the paper found that the corrected slip coefficient may decrease with wall stress. This behaviour might have occurred due to the short residence time of the foam in the rheometer, resulting in incomplete formation of the boundary layer or insufficient time for microstructural adjustments to take place. It is also possible that the boundary layer becomes intermittently damaged by collision of bubbles with the walls at high shear rates.

The general results of this paper are applicable to fire-fighting foams, however, there are a few important points that need to be made. In our experiments, care is taken to keep all variables, e.g. surface tension, bubble size and liquid phase viscosity constant throughout. The actual results obtained here, for example the power-law constants k and n, are only applicable for the foam produced in our experiments. Hence, when using a different surfactant solution and concentration or a different foam generation mechanism, a new master curve must first be established to characterise the new foam type. Further considerations are needed when applying these results to the flow of foams through long pipe lengths, as typically required for fire fighting. The effect of changing foam structure and drainage of liquid from the foam while foam is in pipe transit is not accounted for by this method. Further research needs to be carried out on the formation of the wall slip liquid layer and its evolution with bulk foam properties along a pipe.

Acknowledgement

The authors wish to thank the Australian Research Council for providing financial support for the present work.

References

[1] Schaefer T. 3M Australia, Personal Communication, 1995.
[2] Liebson J. Introduction to Class A Foams and Compressed Air Systems for the Structural Fire Service. Ashland: ISFSI, 1991.
[3] NFPA 412, Standard for Evaluating Aircraft Rescue and Fire Fighting Foam Equipment. Quincy: NFPA, 1993.
[4] de Vries AJ. Morphology, coalescence, and size distribution of foam bubbles. In: Lemlich R, editor. Adsorptive Bubble Separation Techniques, Ch. 2. New York: Academic Press, 1972.
[5] Princen H. Rheology of foams and highly concentrated emulsions: 1. Elastic properties and yield stress of a cylindrical model system. J Colloid Interf Sci 1983;91:160–175.
[6] Bikerman JJ, Foams. New York: Springer, 1973.
[7] Khan S, Armstrong R. Rheology of foams: I. Theory of dry foams. J Non-Newt Fluid Mech 1986;22:1–22.
[8] Hoffer MS, Rubin E. Flow regimes of stable foams. I&EC Fund. 1969;8:483–90.
[9] Heller J, Kuntamukkula M, Critical review of foam rheology literature. Ind Eng Chem Res 1987;26:318–25.
[10] Enzendorfer C, Harris R, Valkó P, Economides M, Fokker P, Davies D. Pipe viscometry of foams. J Rheol 1995;39:345–58.
[11] Cohen Y. Apparent slip flow of polymeric solutions. In: Chereminisoff NP, editor. Encyclopedia of Fluid Mechanics, Vol. 7, Ch. 14. Houston, 1986.
[12] Jastrzebski Z. Entrance effect and wall effects in an extrusion rheometer during the flow of concentrated suspensions. Ind Eng Chem Res 1967;6:445–54.
[13] Valkó P. Economides M, Volume equalised constitutive equations for foamed polymer solutions. J Rheol 1992;36:1033–055.
[14] Durian DJ, Weitz DA, Pine DJ. Scaling behaviour in shaving cream. Phys. Rev. A 1991; 44:R7902–905.
[15] Oldroyd JG. The interpretation of observed pressure gradients in laminar flow of non-Newtonian liquids through tubes. Colloid Sci 1949;4:333–42.
[16] Mooney M. Explicit formulas for slip and fluidity. J Rheol 1931;2:210–22.
[17] Macosko CW. Rheology: Principles, Measurements, and Applications. New York: VCH, 1994.
[18] Prud'homme R, Khan S. Experimental results on foam rheology. In: Prud'homme R, Khan S, editors. FOAMS: Theory, Measurements, and Applications, Ch. 4. New York: Marcel Dekker, 1996.
[19] Pithia KD, Edwards SF. Rheology of liquid foams. Physica A 1994;205:565–76.
[20] Massey BS. Mechanics of Fluids, 5th edn. Wokingham: Van Nostrand Reinhold (UK), 1983.
[21] Bird RB, Steward WE, Lightfoot EN. Transport Phenomena. New York: John Wiley, 1960.